



Efficient separation of alumina and silica in reduction-roasted kaolin by alkali leaching

Xiao-bin LI, Hong-yang WANG, Qiu-sheng ZHOU, Tian-gui QI, Gui-hua LIU, Zhi-hong PENG, Yi-lin WANG

School of Metallurgy and Environment, Central South University, Changsha 410083, China

Received 23 December 2017; accepted 2 May 2018

Abstract: Alkali leaching was employed to investigate the separation of alumina and silica in roasted kaolin obtained by roasting kaolin alone in air at 1273 K for 60 min and in clinker prepared by roasting the mixed raw meal of kaolin, ferric oxide and coal powder with $\text{Fe}_2\text{O}_3/\text{Al}_2\text{O}_3/\text{C}$ molar ratio of 1.2:2.0:1.2 in reducing atmosphere at 1373 K for 60 min. The thermodynamic analyses and alkali leaching results show that the composition of the Al–Si spinel in roasted kaolin is close to that of $3\text{Al}_2\text{O}_3 \cdot 2\text{SiO}_2$ and the spinel is dissolved with increasing leaching time, resulting in difficulty in deeply separating alumina and silica in kaolin by the traditional roasting–leaching process. On the contrary, the efficient separation of alumina and silica in kaolin can be reached by fully converting kaolinite into insoluble hercynite and soluble free silica, namely quartz solid solution and cristobalite solid solution, during reduction roasting, followed by alkali leaching of the obtained clinker. Furthermore, experimental results from treating high-silica diasporic bauxite indicate that the reduction roasting–alkali leaching process is potential to separate silica and alumina in aluminosilicates.

Key words: kaolin; Al–Si spinel; hercynite; high-silica diasporic bauxite; reduction roasting; alkali leaching

1 Introduction

World bauxite reserves include large amounts of ores which at present are sub-economic due to high levels of reactive silica. As the economic reserves of high grade ores diminish, much attention has been paid to pre-separation of silica from low A/S (mass ratio of alumina to silica) bauxite in order to offer qualified raw materials for the Bayer alumina refinery. Several typical methods have been proposed for the pretreatment of bauxite, such as flotation dressing [1–4], direct wet treatment [5] and roasting–leaching process [6–8]. Among these, only flotation dressing has been applied in industry, in which part silicon-containing minerals and diasporic are separated and the A/S in concentrate can increase to 8–10 from 5–6 in raw bauxite [2,4]. However, the alumina recovery in the beneficiation process is only about 85% for the raw bauxite with A/S of 5–6 and tends to decrease remarkably with the A/S decreasing [1], resulting in being unsuitable for treating low A/S bauxite. As to the direct wet treatment method, it is complicated and only suitable to treat kaolinite in bauxite, although

high alumina recovery and relatively high A/S concentrate can be obtained by dissolving aluminosilicates in alkali solution [5].

As another potential pre-desilication method, roasting–leaching process [6–8] is proposed to handle bauxite with high silica for comprehensive utilization of silica and alumina in aluminosilicates [9]. During the roasting, kaolinite firstly dehydrates at about 550 °C and then splits into amorphous silica and cubic phase at about 980 °C. After that, the amorphous silica and cubic phase can be separated by alkali leaching. However, there are disputes in cubic phase i.e. $\gamma\text{-Al}_2\text{O}_3$ [6,10,11] or Al–Si spinel [12–16], which affects the leaching rate of amorphous silica. Actually, alkali leaching results [14,15] prove that the composition of cubic phase is nearly equal to that of $3\text{Al}_2\text{O}_3 \cdot 2\text{SiO}_2$. In other words, the amount of amorphous silica liberated from kaolinite at 980 °C is 66.67% at most.

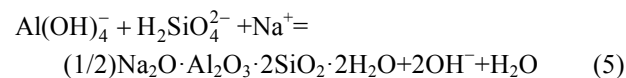
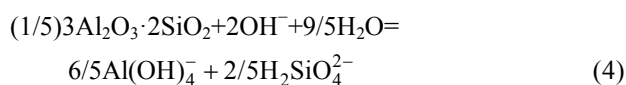
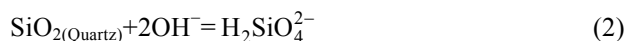
In order to develop a new process for efficiently realizing the separation of alumina and silica in kaolinite, LI et al [17] have introduced ferric oxide-involved reduction roasting process, which involves fully converting kaolinite into hercynite and free silica,

namely quartz solid solution and cristobalite solid solution, during reduction roasting in order to avoid Al–Si spinel (mullite) formation. Based on thermodynamic analysis for reactions in alkali leaching of roasted kaolin obtained by roasting kaolin alone in air at 1273 K for 60 min and in clinker prepared by roasting the mixed raw meal of kaolin, ferric oxide and carbon with $\text{Fe}_2\text{O}_3/\text{Al}_2\text{O}_3/\text{C}$ molar ratio of 1.2:2.0:1.2 in reducing atmosphere at 1373 K for 60 min, the separation of alumina and silica was carried out in alkali solution, and the residues were further examined by XRD and SEM–EDS. Additionally, high-silica diasporic bauxite was chosen to verify the feasibility of treating low A/S bauxite by the reduction roasting–alkali leaching process (RRALP).

2 Thermodynamic analysis

Although large amounts of alkali leaching results about roasting–leaching process [6,8,18] were published, theoretical analysis of alkali leaching was seldom reported. Besides, the separation of hercynite and free silica in clinker by alkali leaching is not known yet in theory. Thus, it is necessary to carry out thermodynamic analysis on reactions of roasted kaolin or clinker during alkali leaching.

The possible reactions were listed in Eqs. (1)–(6) with dissolution in alkali solution. In convenience of comparison, the stoichiometric coefficient of OH^- was normalized to be 2.



The calculated relationships between standard Gibbs free energy change ΔG_T^\ominus and temperature T for the reactions were plotted in Fig. 1, in which the thermodynamic data were derived from Refs. [19–22].

Thermodynamically, the breakdown products of kaolinite at 980 °C, amorphous silica and cubic phase ($\gamma\text{-Al}_2\text{O}_3$ or mullite), are readily soluble in alkali solution because the ΔG_T^\ominus values of Reactions (1)–(4) are negative. Once there are enough silicate anions and aluminate ions in alkali solution, the formation of desilication products (DSP) can occur spontaneously by Reaction (5) due to the negative ΔG_T^\ominus . Thus, the

efficient separation of alumina and silica in kaolinite cannot be obtained by the roasting–leaching process. On the contrary, hercynite is unable to react with alkali solution according to Reaction (6) due to the positive ΔG_T^\ominus , meaning that efficient separation of alumina and silica in kaolinite could be obtained by RRALP.

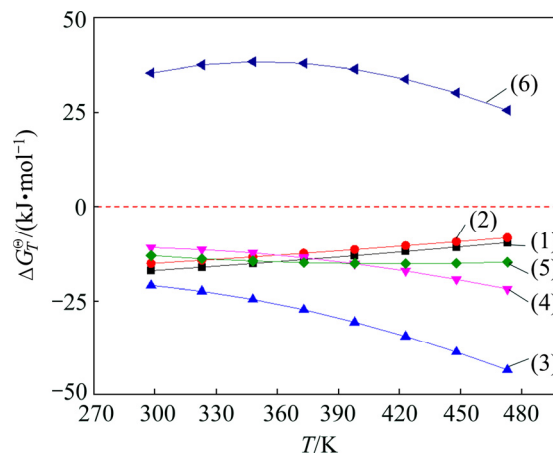


Fig. 1 Relationships between ΔG_T^\ominus and T for Eqs. (1)–(6)

3 Experimental

3.1 Experimental materials

Both Fe_2O_3 ($d_{50}=2.80 \mu\text{m}$) and NaOH are in analytical grade, while coal powder used as the reductant has a fixed carbon of 76.47%. The kaolin sample ($d_{50}=2.82 \mu\text{m}$) used in this investigation was purchased from Guangdong, China, and roasted alone in air at 1273 K for 60 min to obtain roasted kaolin. The sample of clinker was prepared by roasting raw meal of kaolin, ferric oxide and coal powder with $\text{Fe}_2\text{O}_3/\text{Al}_2\text{O}_3/\text{C}$ molar ratio of 1.2:2.0:1.2 in reducing atmosphere at 1373 K for 60 min [17]. High-silica diasporic bauxite was provided by Henan Branch of CHALCO. The structural characterization of kaolin, roasted kaolin, clinker and high-silica diasporic bauxite was determined by X-ray diffractometer (TTR-III, Rigaku Corporation, Japan) with $\text{Cu K}\alpha$ radiation ($\lambda=1.5406 \text{ \AA}$). Data were recorded for 2θ from 10° to 80° and 0.02° step size was used at a scan rate of $10^\circ/\text{min}$.

3.2 Experimental procedures

The leaching experiments were carried out in glycerol cell (XYF–d44×6, machinery plant affiliated to Central South University, China). The roasted kaolin and clinker were separately ground by vibrating mill to granularity with particle size $<74 \mu\text{m}$, and a certain quantity of sample was leached with 160 g/L NaOH solution in a 150 mL sealed rotating steel reactor immersed in glycerol cell at a preset temperature of 383 K. In order to strengthen stirring, $2 \times d18 \text{ mm}$ and $2 \times d8 \text{ mm}$ steel balls were added into the reactor in

advance. After reaction, the reactor was taken out of the cell and then immediately cooled in tap water. The obtained slurry was subsequently filtered to obtain the leachate and leached residue for further analyses.

The phase analysis of leached residues was also performed on powder using the X-ray diffractometer. Surface microscopic morphology and micro area composition analyses were conducted by SEM (JSM–6360LV, JEOL, Japan) and EDS (GENSIS60S, EDAX, USA). The Al_2O_3 , SiO_2 and Na_2O contents in the leachate and leached residue were measured by the EDTA volumetric method, molybdenum blue colorimetry with visible spectrophotometer (L2, INESA, China) and flame photometer (AP1302, AOPU, China), respectively. The leaching rate of silica ($\eta(\text{SiO}_2)$) in clinker was calculated using the following formula:

$$\eta(\text{SiO}_2) = \frac{m_1 w_1(\text{SiO}_2) - m_2 w_2(\text{SiO}_2)}{m_1 w_1(\text{SiO}_2)} \times 100\% \quad (7)$$

where $w_1(\text{SiO}_2)$ and $w_2(\text{SiO}_2)$ represent mass fractions of silica for the clinker and leached residue respectively, while m_1 and m_2 denote the masses of the clinker and leached residue, respectively.

4 Results and discussion

4.1 Characterization of materials

The chemical compositions of kaolin, roasted kaolin, clinker and high-silica diasporic bauxite are shown in Table 1. The major chemical compositions in kaolin are Al_2O_3 and SiO_2 , accounting for 37.09% and 45.10%, respectively. Moreover, other impurities, such as Fe_2O_3 , TiO_2 and K_2O , are also observed in small quantities and the quartz content in kaolin is about 1.46% calculated by A/S. After roasting at 1273 K for 60 min, the chemical compositions in roasted kaolin significantly increase compared with those in kaolin for dehydration. As for the clinker, besides Al_2O_3 and SiO_2 , Fe_2O_3 is also one of the major chemical compositions. In high-silica diasporic bauxite, the A/S is 3.65 with 59.53% Al_2O_3 and 16.30% SiO_2 .

The X-ray diffraction patterns of kaolin, roasted kaolin, clinker and high-silica diasporic bauxite are shown in Fig. 2. The main diffraction peaks in the pattern indicate that kaolin (Fig. 2(a)) mainly consists of kaolinite and a small amount of quartz. After roasting at 1273 K for 60 min, quartz and anatase remain unchanged in roasted kaolin (Fig. 2(b)), but the characteristic diffraction peaks of kaolinite disappear, which means that the kaolinite converts to amorphous states involving free silica and cubic phase. Figure 2(c) indicates that the complete conversion of kaolinite into free silica, namely quartz solid solution and cristobalite solid solution, and hercynite can be achieved by roasting kaolin with ferric

oxide in reducing atmosphere. As shown in Fig. 2(d), high-silica diasporic bauxite contains diasporite, kaolinite, quartz, hematite, anatase and illite.

Table 1 Chemical compositions of kaolin, high-silica bauxite, roasted kaolin and clinker (wt.%)

Sample	Al_2O_3	SiO_2	Fe_2O_3	TiO_2	K_2O	A/S
Kaolin	37.09	45.10	0.83	0.98	0.28	0.82
Roasted kaolin	40.76	50.51	0.96	1.11	0.31	0.81
Clinker	32.69	40.46	28.59	0.78	0.24	0.81
High-silica bauxite	59.53	16.30	6.81	3.00	1.10	3.65

4.2 Separation of alumina and silica by alkali leaching

4.2.1 Roasted kaolin

The composition of Al–Si spinel can be calculated by leaching rate of amorphous silica treated with dilute NaOH solution; however, the major problem arises in determining the end-point, particularly of NaOH solution-free amorphous SiO_2 reaction in the presence of other reactions [15]. Therefore, a method was proposed in this work to deduce the composition of Al–Si spinel by A/S in the leached residue calculated in the following way. The total percentages of $\text{Al}_2\text{O}_3(\text{T})$, $\text{SiO}_2(\text{T})$ and $\text{Na}_2\text{O}(\text{T})$ in residue were firstly analyzed. Based on the amount of $\text{Na}_2\text{O}(\text{T})$, the corresponding amounts of $\text{Al}_2\text{O}_3(\text{S})$ and $\text{SiO}_2(\text{S})$ in DSP were calculated according to the formula of DSP. Meanwhile, the $\text{SiO}_2(\text{Q})$ content in residue could also be calculated provided that natural quartz is inactive in NaOH solution at atmospheric pressure. Subsequently, the Al_2O_3 content in Al–Si spinel can be calculated by subtracting $\text{Al}_2\text{O}_3(\text{S})$ content from $\text{Al}_2\text{O}_3(\text{T})$ content, similarly, the SiO_2 content in Al–Si spinel can be calculated by subtracting $\text{SiO}_2(\text{S})$ content and $\text{SiO}_2(\text{Q})$ content from $\text{SiO}_2(\text{T})$ content. Therefore, the A/S ratio in Al–Si spinel is obtained. In order to decrease the influence of DSP, the alkali leaching of roasted kaolin was carried out with a solid/liquid ratio of 1:100 g/mL at 373 K and the results are shown in Table 2.

The residue mass changes from 0.55 g at leaching time of 20 min to 0.36 g at time of 90 min followed by 0.63 g for 180 min, indicating precipitation of sodalite (shown in Fig. 3) by silicate anions reacting with aluminate ions in solution. The sodalite formation can be confirmed by the increase of $\text{Na}_2\text{O}(\text{T})$ content, as well as the decrease of Al_2O_3 content in the residue with leaching time. Despite the influence of quartz and sodalite, the $(\text{A/S})_2$ in residue is stable at about 2.65, which is close to that of $3\text{Al}_2\text{O}_3 \cdot 2\text{SiO}_2$ (A/S=2.55). Therefore, the composition of the Al–Si spinel is close to that of mullite of $3\text{Al}_2\text{O}_3 \cdot 2\text{SiO}_2$.

The XRD patterns of the residues obtained by leaching roasted kaolin are shown in Fig. 3. It can be

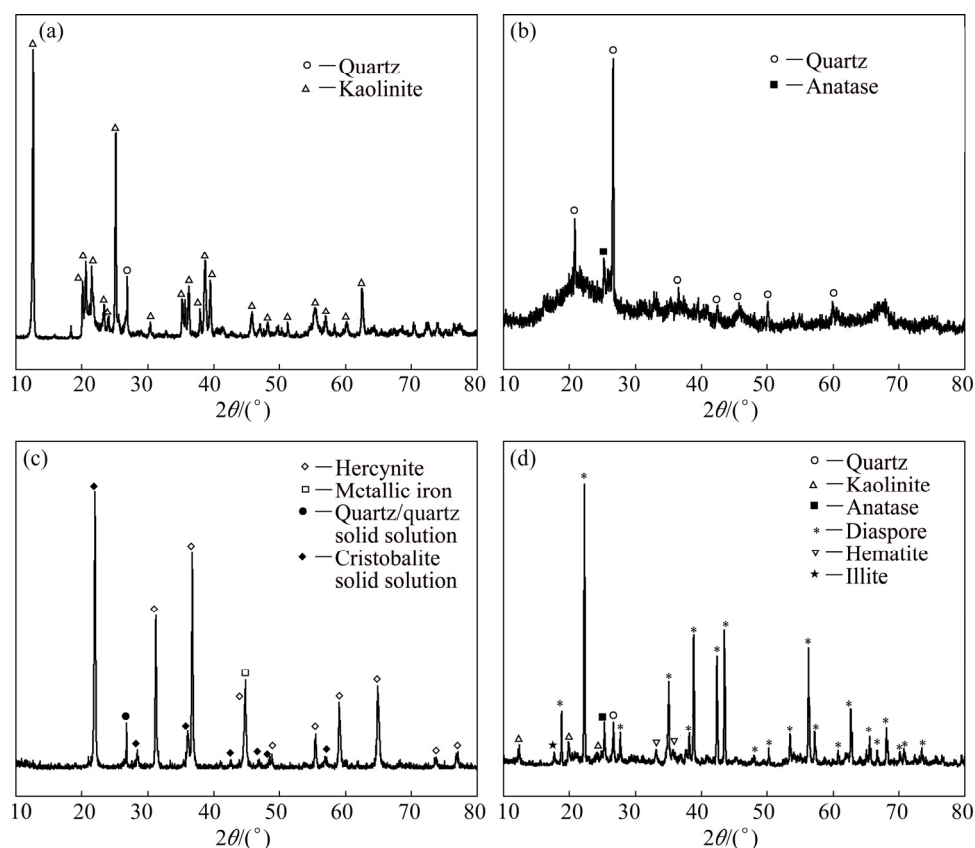


Fig. 2 XRD patterns of kaolin (a), roasted kaolin(b), clinker (c) and high-silica bauxite(d)

Table 2 Leaching results of roasted kaolin in alkali solution

Time/min	Mass/g	Mass fraction in residue/%						(A/S) ₁	(A/S) ₂
		Al ₂ O _{3(T)}	SiO _{2(T)}	Na ₂ O _(T)	Al ₂ O _{3(S)}	SiO _{2(S)}	SiO _{2(Q)}		
20	0.55	53.72	25.75	0.54	0.67	0.78	2.97	2.09	2.41
60	0.38	53.68	25.42	0.96	1.18	1.39	4.21	2.11	2.65
90	0.36	53.20	25.32	1.19	1.47	1.73	4.48	2.10	2.71
120	0.44	53.78	25.92	1.76	2.17	2.55	3.63	2.07	2.62
180	0.63	51.18	30.29	8.62	10.64	12.51	2.53	1.69	2.66

Al₂O_{3(T)}, SiO_{2(T)} and Na₂O_(T): Total contents of Al₂O₃, SiO₂ and Na₂O in residue, respectively; Al₂O_{3(S)}, SiO_{2(S)}: Al₂O₃ and SiO₂ contents of sodalite in residue, respectively; SiO_{2(Q)}: Quartz content in residue; (A/S)₁=w(Al₂O_{3(T)})/w(SiO_{2(T)}); (A/S)₂=[w(Al₂O_{3(T)})-w(Al₂O_{3(S)})]/[w(SiO_{2(T)})-w(SiO_{2(S)})-w(SiO_{2(Q)})]

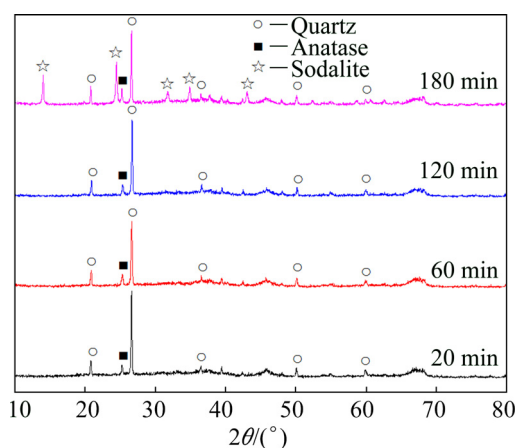


Fig. 3 XRD patterns of residues obtained by leaching roasted kaolin (Leaching conditions: 383 K, NaOH concentration 160 g/L, solid/liquid ratio 1: 100 g/mL)

seen that sodalite cannot form unless leaching time is over 180 min with solid/liquid ratio of 1:100 g/mL, which indicates that the dissolution of amorphous silica is prior to that of Al–Si spinel of $3\text{Al}_2\text{O}_3 \cdot 2\text{SiO}_2$ and the spinel is dissolved by Eq. (4) with leaching time, thus causing the formation of sodalite by silicate anions reacting with aluminate ions in solution according to Eq. (5).

The leaching residues were further analyzed by SEM–EDS under the same leaching condition of Fig. 3 to investigate the formation of sodalite. As shown in Figs. 4(a₁) and (b₁), the particles in residue obtained by leaching roasted kaolin for 60 min remain platelike structure, and no sodalite is formed as sodium is not found in Fig. 4(b₁) for Points 1 and 2 in the inset of Fig. 4(a₁) by analyzing with EDS. In addition, the silicon

contents at Points 1 and 2 significantly decrease, which shows that amorphous silica is readily soluble in alkali solution. When leaching time increases to 180 min, irregular spherical particles can be discovered in the leaching residue besides platelike particles from Fig. 4(a₂). The presence of sodium in Fig. 4(b₂) for Points 3 and 4 indicates the formation of sodalite, being in agreement with the results of both alkali leaching and XRD analysis. So, we can draw a conclusion that, the efficient separation of alumina and silica in kaolinite cannot be obtained by the traditional roasting–leaching process mainly due to the formation of Al–Si spinel of $3\text{Al}_2\text{O}_3 \cdot 2\text{SiO}_2$ during the roasting as well as the formation of DSP during the alkali leaching.

4.2.2 Reduction-roasted kaolin

In general, natural minerals such as hercynite,

quartz and cristobalite are difficult to dissolve in dilute alkali solution at atmospheric pressure, while the amorphous silica decomposed from kaolinite by the traditional roasting is readily soluble as mentioned in Section 4.2.1. Nevertheless, there is doubt that the quartz solid solution and cristobalite solid solution are able to dissolve in such a system. Thus, the separation of alumina and silica in clinker was conducted experimentally in alkali solution and the results are shown in Table 3.

The A/S in the leached residue of the clinker consistently increases with increasing leaching time, implying that less DSP is formed. Very low Al_2O_3 concentration (~ 0.1 g/L) in the leachate and Na_2O content ($< 0.5\%$) in the residue suggest that the poor reactivity of alumina in hercynite (Eq. (6)), and secondary reaction to form DSP does not occur seriously

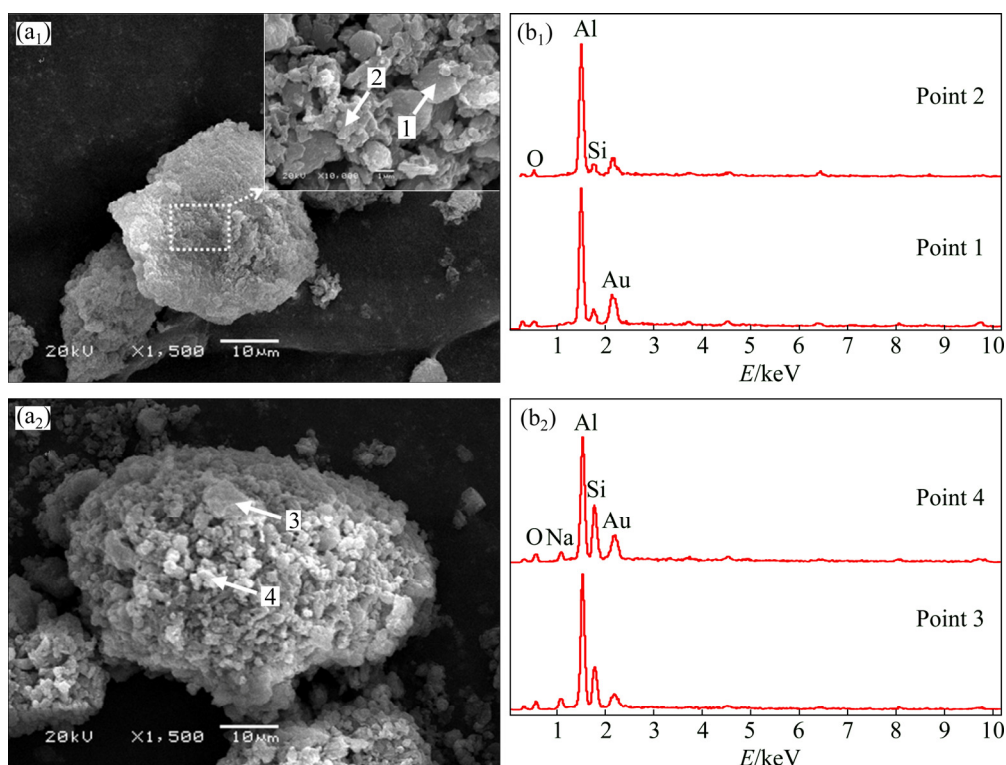


Fig. 4 SEM images (a₁, a₂) and EDS patterns (b₁, b₂) of residue obtained by leaching roasted kaolin for 60 min (a₁, b₁) and 180 min (a₂, b₂) (Leaching conditions: 383 K, NaOH concentration 160 g/L, solid/liquid ratio 1:100 g/mL)

Table 3 Leaching results of clinker in alkaline solution at 383 K and NaOH concentration of 160 g/L

Solid/liquid ratio/(g·mL ⁻¹)	Leaching time/min	Concentration of leachate/(g·L ⁻¹)		Mass of residue/g	Mass fraction in residue/%			A/S
		Al ₂ O ₃	SiO ₂		Al ₂ O ₃	SiO ₂	Na ₂ O	
5:50	20	0.08	24.50	3.94	38.38	18.26	0.21	2.10
	60	0.11	32.48	3.36	45.69	8.87	0.36	5.15
	120	0.12	34.60	3.27	47.67	5.86	0.38	8.13
7:50	20	0.08	28.15	5.50	38.44	23.06	0.24	1.67
	60	0.10	45.22	4.76	44.41	9.34	0.31	4.75
	120	0.10	48.16	4.52	46.77	5.92	0.41	7.90

Clinker: Roasting raw meal with $\text{Fe}_2\text{O}_3/\text{Al}_2\text{O}_3/\text{C}$ molar ratio of 1.2:2.0:1.2 at 1373 K for 60 min

in the alkali leaching process, which yields Al_2O_3 recovery of almost 100% in the concentrate. This can also be proved by the decreasing trend of residue mass and increasing trend of SiO_2 concentration (28–50 g/L) with increasing time.

To attest the abovementioned discussion, the leaching residues were analyzed by XRD. As shown in Fig. 5, no new substance is detected in residues after leaching for 60 min besides hercynite, quartz/quartz solid solution and metallic iron which already exist in clinker. Meanwhile, the characteristic peaks of cristobalite solid solution vanish and the peak intensity of quartz/quartz solid solution reduces, which confirms that both cristobalite solid solution and quartz solid solution are readily soluble in alkali solution at atmospheric pressure. The fact that diffraction apex of quartz/quartz solid solution at 2θ of 26.6° reduces but still remains in the leaching residues indicates that quartz solid solution has similar characteristic peaks and dissimilar leaching performance in alkali solution to quartz. The XRD analyses agree with those of leaching experiments.

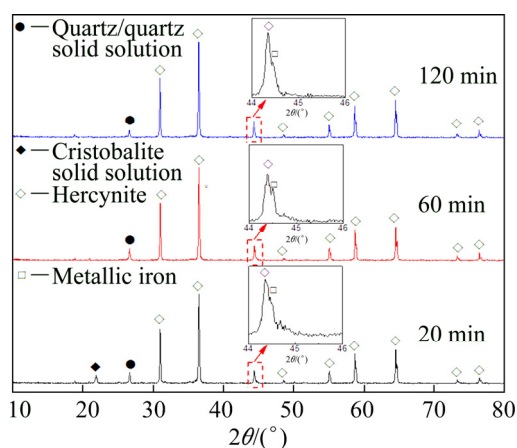


Fig. 5 XRD patterns of residues obtained by leaching clinker (Leaching conditions: 383 K, NaOH concentration 160 g/L, solid/liquid ratio 5: 50 g/mL)

In order to find the existing form of silica, the leaching residue of clinker was further studied by SEM–EDS, and the results are shown in Fig. 6. The SEM image of leaching residue shows a surface with an abundance of extremely small (submicron) particles like flecks located on or slightly embedded in the surface, while only a small amount of micropores can be observed in the interior of leaching residue particle. The EDS results of Point 1 in Fig. 6(a) indicate that the independent natural quartz introduced from kaolin neither reacts with ferrous oxide under the reduction roasting condition, nor dissolves in alkali solution at atmospheric pressure. However, there is a large amount of silicon but a small amount of iron in the interior of leaching residue particle as shown at Point 2 (in

Fig. 6(a)), which may be caused by direct decomposition of kaolinite at 1373 K due to the local inhomogeneous composition. Besides the main elements of oxygen, aluminum and iron, a small amount of silicon is also detected in leached hercynite particle (Point 3 in Fig. 6(a)), which can be explained by the fact that a certain portion of silica is wrapped by hercynite during reduction roasting. In addition, no DSP is formed during the alkali leaching as sodium is not detected on the surface of the leaching residue, being in accordance with the analysis results of Na_2O content in residue listed in Table 3. Thus, the diffraction peak at 2θ of 26.6° in the leaching residue is contributed to both quartz and quartz solid solution.

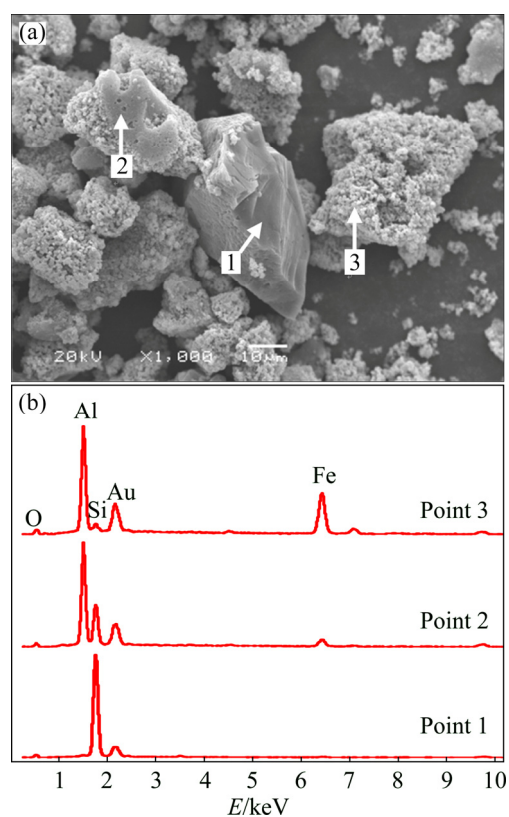


Fig. 6 SEM image (a) and EDS pattern (b) of residue obtained by leaching clinker for 120 min (Leaching conditions: 383 K, NaOH concentration 60 g/L, solid/liquid ratio 5:50 g/mL)

In short, the efficient separation of alumina and silica in kaolinite can be achieved by fully converting kaolinite into insoluble hercynite and soluble free silica, namely quartz solid solution and cristobalite solid solution, during reduction roasting, followed by alkali leaching of the obtained clinker.

4.3 Experimental validation of high-silica bauxite

To evaluate the feasibility of RRALP for application in alumina industry, experiments were carried out by using high-silica diasporic bauxite. The differences in

silica leaching rates in alkali solution and A/S in residue were measured between the bauxite clinker obtained by the reduction roasting at 1373 K for 60 min [17] and the roasted bauxite obtained by roasting bauxite alone in air at 1273 K for 60 min. Results are demonstrated in Figs. 7 and 8.

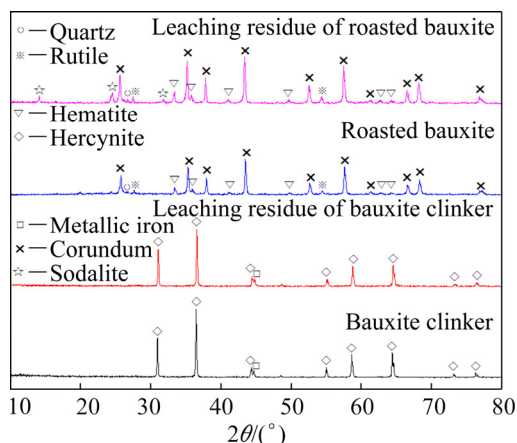


Fig. 7 XRD patterns of bauxite clinker, roasted bauxite and their corresponding leaching residues (Roasted bauxite: roasting bauxite alone in air at 1273 K for 60 min; Bauxite clinker: roasting raw meal with $\text{Fe}_2\text{O}_3/\text{Al}_2\text{O}_3/\text{C}$ molar ratio of 1.2:2.0:1.2 in reducing atmosphere at 1373 K for 60 min; Leaching conditions: 180 min, 383 K, NaOH concentration 160 g/L, solid/liquid 5: 50 g/mL)

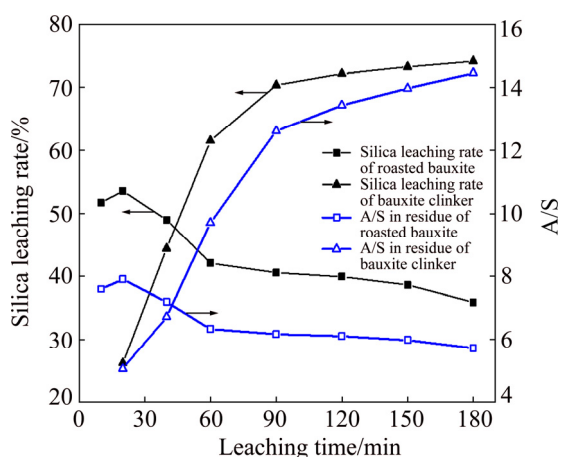


Fig. 8 Effect of leaching time on silica leaching rate and A/S in residue for roasted bauxite and bauxite clinker (Leaching conditions: 383 K, NaOH concentration 160 g/L, solid/liquid 5:50 g/mL)

As shown in Fig. 7, hematite, corundum, rutile and quartz can be found in roasted bauxite, while only hercynite and metallic iron can be detected in bauxite clinker by XRD due to either poor crystallinity or too low content for other substances. The leaching results of roasted bauxite (Fig. 8) indicate that both silica leaching rate and A/S in residue simultaneously reach the maximum of about 55% and 8 after leaching for 20 min,

and then decrease with increasing leaching time due to sodalite formation (Fig. 7). However, when the bauxite clinker is leached under the same conditions, less DSP is formed because the silica leaching rate and A/S in residue only increase with the increase of leaching time, which can also be confirmed by XRD (Fig. 7). In RRALP, the silica leaching rate of 75% and A/S of above 14 can be available after leaching for 180 min, which shows its great potential in pre-treating high-silica bauxite. It should be noted that, the unreacted diasporite is transformed into corundum at 1373 K, while the silica existing in leaching residue of bauxite clinker is mainly in the form of quartz (Fig. 9), meaning that the natural quartz in bauxite cannot be dissolved by RRALP. So, it is necessary to further study how to efficiently activate quartz for further improving silica leaching rate during alkali leaching in the future.

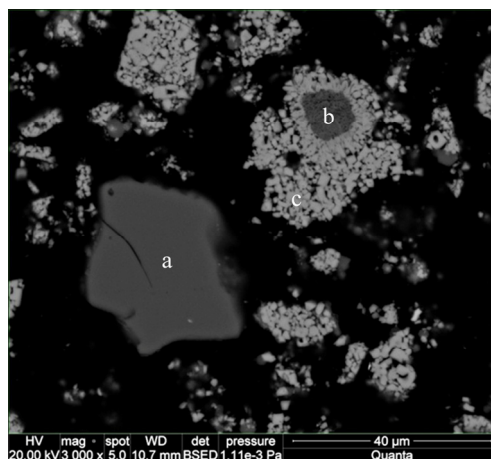


Fig. 9 SEM image of residue obtained by leaching bauxite clinker for 180 min (a—Quartz; b—Corundum; c—Hercynite; Leaching conditions: 383 K, NaOH concentration 160 g/L, solid/liquid ratio 5:50 g/mL)

5 Conclusions

(1) Alkali leaching results of roasted kaolin indicate that the composition of the Al–Si spinel decomposed from kaolinite at 1273 K is close to that of mullite of $3\text{Al}_2\text{O}_3 \cdot 2\text{SiO}_2$, and the spinel can further react with alkali solution with leaching time.

(2) In treating the clinker by alkali solution under atmospheric pressure, hercynite is rather inactive but quartz solid solution/cristobalite solid solution is readily soluble, leading to an efficient separation of alumina and silica in kaolin by RRALP.

(3) When treating high-silica diasporic bauxite with A/S of 3.65 by RRALP, the A/S in concentrate can reach 14.15 and almost no alumina is dissolved during alkali leaching of silica, manifesting that RRALP is promising to pre-treat Al/Fe-bearing materials with high silica for alumina production.

References

- [1] HU Y, LIU X, XU Z H. Role of crystal structure in flotation separation of diasporite from kaolinite, pyrophyllite and illite [J]. Minerals Engineering, 2003, 16: 219–227.
- [2] WANG Y, HU Y, HE P, GU G. Reverse flotation for removal of silicates from diasporic-bauxite [J]. Minerals Engineering, 2004, 17: 63–68.
- [3] XIA Liu-yin, ZHONG Hong, LIU Guang-yi, HUANG Zhi-qiang, CHANG Qing-wei. Flotation separation of the aluminosilicates from diasporite by a Gemini cationic collector [J]. International Journal of Mineral Processing, 2009, 92: 74–83.
- [4] XU Zheng-he, PLITT V, LIU Qi. Recent advances in reverse flotation of diasporic ores—A Chinese experience [J]. Minerals Engineering, 2004, 17: 1007–1015.
- [5] LIU Gui-hua, LI Xiao-bin, PENG Zhi-hong, ZHANG Chuan-fu, HE Bo-quan. Advances in wet pretreatment of bauxite [J]. Mining and Metallurgical Engineering, 2000, 20(3): 55–58. (in Chinese)
- [6] QIU Guan-zhou, JIANG Tao, LI Guang-hui, FAN Xiao-hui, HUANG Zhu-cheng. Activation and removal of silicon in kaolinite by thermochemical process [J]. Scandinavian Journal of Metallurgy, 2004, 33: 121–128.
- [7] BONN H S, GINSBERG H. Method for reducing the silica content of alumina-containing materials of the clay type: US patent, 2939764 [P]. 1960–06–07.
- [8] RAYZMAN V L, PEVZNER I Z, SIZYAKOV V M, NI L P, FILIPOVICH I K, ATURIN A V. Extracting silica and alumina from low-grade bauxite [J]. The Journal of the Minerals, Metals & Materials Society, 2003, 55: 47–50.
- [9] SMITH P. The processing of high silica bauxites—Review of existing and potential processes [J]. Hydrometallurgy, 2009, 98: 162–176.
- [10] PERCIVAL H J, DUNCAN J F, FOSTER P K. Interpretation of the kaolinite–mullite reaction sequence from infrared absorption spectra [J]. Journal of the American Ceramic Society, 1974, 57(2): 57–61.
- [11] SONUPARLAK B, SARIKAYA M, AKSAY I A. Spinel phase formation during the 980 °C exothermic reaction in the kaolinite-to-mullite reaction series [J]. Journal of the American Ceramic Society, 1987, 70(11): 837–842.
- [12] SANZ J, MADANI A, SERRATOSA J M. Aluminum-27 and silicon-29 magic-angle spinning nuclear magnetic resonance study of the kaolinite–mullite transformation [J]. Journal of the American Ceramic Society, 1988, 71(10): C418–C421.
- [13] SRIKRISHNA K, THOMAS G, MARTINEZ R, CORRAL M P, DEAZA S, MOYA J S. Kaolinite–mullite reaction series: A TEM study [J]. Journal of Materials Science, 1990, 25: 607–612.
- [14] CHAKRABORTY A K, GHOSH D K. Reexamination of the kaolinite-to-mullite reaction series [J]. Journal of the American Ceramic Society, 1978, 61(3–4): 170–173.
- [15] CHAKRABORTY A K. Supplementary alkali extraction studies of 980 °C-heated kaolinite by X-ray diffraction analysis [J]. Journal of Materials Science, 1992, 27: 2075–2082.
- [16] LEE S, KIM Y J, MOON H S. Phase transformation sequence from kaolinite to mullite investigated by an energy-filtering transmission electron microscope [J]. Journal of the American Ceramic Society, 1999, 82(11): 2841–2848.
- [17] LI Xiao-bin, WANG Hong-yang, ZHOU Qiu-sheng, QI Tian-gui, LIU Gui-hua, PENG Zhi-hong, WANG Yi-lin. Reaction behavior of kaolinite with ferric oxide during reduction roasting [J]. Transactions of Nonferrous Metals Society of China, 2019, 29(1): 186–193.
- [18] JIANG Tao, LI Guang-hui, FAN Xiao-hui, HUANG Zhu-cheng, QIU Guan-zhou. Desilication from diasporic bauxite by roasting-alkali leaching process (I) [J]. The Chinese Journal of Nonferrous Metals, 2000, 10(4): 534–538. (in Chinese)
- [19] BARIN I. Thermochemical data of pure substances [M]. Weinheim: VCH Verlagsgesellschaft mbH, 1995.
- [20] KNACKE O, KUBASCHEWESKI O. Thermodynamic properties of inorganic substances (II) [M]. Heidelberg: Springer-Verlag, 1991.
- [21] YANG Xian-wan, HE Ai-ping, YUAN Bao-zhou. The calculates handbook of high temperature aqueous solution thermodynamics data [M]. Beijing: Metallurgical Industry Press, 1983. (in Chinese)
- [22] LI Xiao-bin, LIU Gui-hua, PENG Zhi-hong, ZHAI Yu-chun. Equilibrium concentration of SiO₂ in aluminate solution [J]. Journal of Northeastern University (Natural Science), 2002, 23(3): 251–254. (in Chinese)

还原焙烧高岭土中氧化铝和氧化硅的碱浸高效分离

李小斌, 王洪阳, 周秋生, 齐天贵, 刘桂华, 彭志宏, 王一霖

中南大学 冶金与环境学院, 长沙 410083

摘要: 分别以 1273 K 单独焙烧 60 min 的高岭土以及高岭土、氧化铁和煤粉(Fe₂O₃/Al₂O₃/C 摩尔比为 1.2:2.0:1.2) 混合物在 1373 K 焙烧 60 min 的还原产物为研究对象, 对焙烧产物中氧化铝和氧化硅的碱浸分离进行研究。热力学计算和碱浸实验结果表明, 热活化高岭土中铝硅晶石的化学成分接近于 3Al₂O₃·2SiO₂, 且随着浸出时间的延长而进一步溶解, 从而使传统焙烧–碱浸法难以实现高岭土中氧化铝和氧化硅的高效分离。相反, 通过添加氧化铁还原焙烧, 将高岭土中氧化铝和氧化硅分别转变为铝酸亚铁和氧化硅固溶体(石英固溶体和方石英固溶体), 通过碱浸则可以实现还原焙烧高岭土中氧化铝和氧化硅的高效分离。高硅–水硬铝石型铝土矿碱浸实验结果进一步表明, 还原焙烧–碱浸法更有利于铝硅酸盐矿物中氧化铝和氧化硅的分离。

关键词: 高岭土; 铝硅晶石; 铝酸亚铁; 高硅–水硬铝石型铝土矿; 还原焙烧; 碱浸

(Edited by Wei-ping CHEN)